Critical Role for Phosphatidylinositol-3 Kinase Vps34/PIK3C3 in ON-Bipolar Cells

Feng He,[1] Ralph M. Nichols,[2] Lavanya Kailasam,[1] Theodore G. Wensel,[1,2] and Melina A. Agosto[1]

[1]Verna and Marrs McLean Department of Biochemistry and Molecular Biology, Baylor College of Medicine, Houston, Texas, United States
[2]Department of Ophthalmology, Baylor College of Medicine, One Baylor Plaza, Houston, Texas, United States

Correspondence: Theodore G. Wensel, Verna and Marrs McLean Department of Biochemistry and Molecular Biology, Baylor College of Medicine, One Baylor Plaza, Houston, Texas 77030, USA; twensel@bcm.edu.

Submitted: January 16, 2019
Accepted: June 3, 2019

Citation: He F, Nichols RM, Kailasam L, Wensel TG, Agosto MA. Critical role for phosphatidylinositol-3 kinase Vps34/PIK3C3 in ON-bipolar cells. *Invest Ophthalmol Vis Sci*. 2019;60:2861–2874. https://doi.org/10.1167/iovs.19-26586

Purpose. Phosphatidylinositol-3-phosphate (PI(3)P), and Vps34, the type III phosphatidylinositol 3-kinase primarily responsible for its production, are important for function and survival of sensory neurons, where they have key roles in membrane processing events, such as autophagy, endosome processing, and fusion of membranes bearing ubiquitinated cargos with lysosomes. We examined their roles in the most abundant class of secondary neurons in the vertebrate retina, the ON-bipolar cells (ON-BCs).

Methods. A conditional Vps34 knockout mouse line was generated by crossing Vps34 floxed mice with transgenic mice expressing Cre recombinase in ON-BCs. Structural changes in the retina were determined by immunofluorescence and electron microscopy, and bipolar cell function was determined by electroretinography.

Results. Vps34 deletion led to selective death of ON-BCs, a thinning of the inner nuclear layer, and a progressive decline of electroretinogram b-wave amplitudes. There was no evidence for loss of other retinal neurons, or disruption of rod-horizontal cell contacts in the outer plexiform layer. Loss of Vps34 led to aberrant accumulation of membranes positive for autophagy markers LC3, p62, and ubiquitin, accumulation of endosomal membranes positive for Rab7, and accumulation of lysosomes. Similar effects were observed in Purkinje cells of the cerebellum, leading to severe and progressive ataxia.

Conclusions. These results support an essential role for PI(3)P in fusion of autophagosomes with lysosomes and in late endosome maturation. The cell death resulting from Vps34 knockout suggests that these processes are essential for the health of ON-BCs.

Keywords: bipolar cell, Vps34, autophagy, phosphoinositide, degeneration

The type III phosphatidylinositol-3 kinase Vps34 (Pik3c3) is critically important for multiple membrane trafficking processes, such as autophagy, phagocytosis, and endocytosis.[1–3] Vps34 is the major producer of phosphatidylinositol-3-phosphate (PI(3)P) by phosphorylation of phosphatidylinositol in the 3-position. PI(3)P in turn recruits proteins to autophagosome and endocytic membranes via PI(3)P-binding FYVE and PX domains.[4–6] Complexes containing Vps34 have important functions in endocytosis and endosome processing, and in the initiation and lysosomal fusion steps in the autophagy pathway.[2,7,8] Vps34 is the only type III phosphatidylinositol-3 kinase in mammals, and is expressed ubiquitously.[9–12] In photoreceptors and other neurons, disruption of Vps34 leads to defects in degradative membrane trafficking, followed by cell death.[13–15]

Bipolar cells (BCs) are the most abundant type of secondary neuron in the retina and are responsible for collecting photoreceptor outputs at synapses in the outer plexiform layer (OPL). The ON-BCs, which depolarize in response to light, include all rod BCs and a subset of cone BCs.[16] As highly polarized neurons, they must sustain a constant flux of membrane material to and from the dendrites where they receive signals from photoreceptor and horizontal cells, as well as rapid turnover of membrane at the synaptic termini where they communicate with downstream neurons. Despite the obvious importance of membrane trafficking in ON-BCs, little is known about how it is regulated or about the roles of phosphoinositides in BCs. Virtually nothing is known about autophagy and endosome processing in these cells. To begin to understand how membranes are trafficked and recycled, we focused on PI(3)P because of its importance in autophagy and endosome processing, as well as in other membrane trafficking events. We generated a conditional Vps34 knockout (KO) line using a Purkinje cell protein-2 (Pcp2)/L7-Cre transgene, which expresses Cre recombinase in rod BCs as well as some types of cone ON and OFF BCs, and Purkinje cells.[17–19] The results revealed that PI(3)P is essential for completion, but not for initiation, of autophagy, as well as for lysosomal fusion with endosomes. As a result, the cells undergo a progressive degeneration, revealing an essential role for these membrane recycling pathways in the survival of these cells.

Materials and Methods

Animals

All animal studies adhered to the ARVO Statement for the Use of Animals in Ophthalmic and Vision Research and were approved by the institutional animal care and use committee at Baylor College of Medicine. Wild type (WT) C57BL/6J (#000664), B6

albino (#000058 B6[Cg])-*Tyr*$^{c-2J}$/J), and Pcp2-Cre (#006207 L7 Cre, Tg[Pcp2-cre] 1Amc/J) mice were purchased from the Jackson Laboratory (Bar Harbor, ME, USA). The Pcp2-Cre mice were found to have the Crb1^{rd8} allele[20] and were crossed with WT C57BL6/J for at least five generations. Although this Pcp2-Cre line was reported by the vendor (Jackson Laboratory) also to express green fluorescent protein (GFP), in retinal bipolar cells or in Purkinje cells in which we could clearly observe Cre immunostaining (Supplementary Fig. S1), we did not observe GFP fluorescence under our imaging conditions using our immunostaining protocol (Supplementary Fig. S2). Vps34 floxed mice (Vps34$^{fl/fl}$), which have loxP sites flanking exons 17 and 18,[13] were a gift from Fan Wang (Duke University); these mixed background C57BL6/129 mice were back-crossed with WT C57BL/6J for at least six generations. Vps34 floxed mice then were bred with Pcp2-Cre mice to generate conditional Vps34 KO mice (Vps34$^{fl/fl}$;Pcp2-Cre). The KO mice suffered from progressive ataxia and generally were euthanized for animal welfare reasons when they developed difficulty in feeding, which usually happened before 10 months of age. Mice with a GFP-LC3 transgene[21] (#RBRC00806, GFP-LC3#53) were obtained from the RIKEN Bio Resource Center (Ibaraki, Japan). Vps34 KO mice also containing transgenic GFP-LC3 (Vps34$^{fl/fl}$;Pcp2-Cre;GFP-LC3$^{+/}$) were generated by crossing Vps34$^{fl/fl}$;Pcp2-Cre mice with the GFP-LC3 transgenic mice. Only mice heterozygous for the GFP-LC3 allele were used.

PCR of tail DNA was used to genotype the Vps34 floxed allele as described,[13] and the Pcp2-Cre transgene was detected using PCR primers 5′-ATTCTCGTGGAACTGGATGG-3′ and 5′-GGACAGGTAATGGTTGTCTGG-3′, per vendor instructions. The GFP-LC3 mice were genotyped with primers A (5′-GGTGTTTGTTCCGTACACATCACC-3′), B (5′-GGCAAAGCGG CAAACAACCATCAC-3′), and C (5′-GAGTGAAGCAGAACGTG GGGCTCACCTCGA-3′), per vendor instructions; primer pairs A+B and A+C detected the WT and transgenic alleles, respectively. The absence of Grm6^{rd1} and Crb1^{rd8} alleles was confirmed by PCR and sequencing as described.[20,22] All mice were maintained in a 12-hour light/12-hour dark cycle (~400 LUX fluorescent illumination during the light cycle) and euthanized by CO_2 inhalation before dissection.

Subretinal Injection and Electroporation of PI(3)P Reporter Plasmid

The hepatocyte growth factor-regulated tyrosine kinase substrate (Hrs) FYVE domain was cloned from mouse kidney mRNA as described,[15] using primers 5′-GAAAGTGATGC CATGTTCGCTGCTGAAAGA-3′ and 5′-TGCCTTCTTGTTCAG CTGCTCATAGCAGGGC-3′. The ON-BC expression plasmids pGrm6P-DsRed and pGrm6P-DsRed-2xHrs, containing the Grm6 promoter 200 base pairs critical region and SV40 enhancer, was derived from Addgene plasmid #18817[23] (a gift from Connie Cepko, Harvard Medical School, Boston, MA, USA) by replacing the GFP-IRES-alkaline phosphatase sequence with DsRed or a fusion of DsRed and two tandem repeats of the Hrs FYVE domain (DsRed-SGGSRRASVGSH-Hrs-QGQGS-Hrs). Subretinal injection and electroporation of plasmid DNA (2–3 mg/mL) in C57BL/6J albino P0 mice were performed as described.[24–26] Injected eyes were processed for confocal microscopy at approximately 4 weeks of age.

Immunostaining and Confocal Microscopy

The following primary antibodies were used for immunostaining. PKCα: mouse monoclonal H-7 (#sc-8393; Santa Cruz Biotechnology, Dallas, TX, USA), rabbit polyclonal (#2056; Cell Signaling Technology, Danvers, MA, USA); PCP2: mouse monoclonal F-3 (#sc-137064; Santa Cruz Biotechnology); calbindin: D28K goat polyclonal (#sc-7691; Santa Cruz Biotechnology), mouse monoclonal CB-955 (#C9848; Sigma-Aldrich Corp., St. Louis, MO, USA); calretinin: mouse monoclonal H-5 (#sc-365956; Santa Cruz Biotechnology); parvalbumin α: goat polyclonal (#sc-7449; Santa Cruz Biotechnology); ribeye: rabbit polyclonal anti-ribeye A-domain (#192-103; Synaptic Systems, Goettingen, Germany); LAMP1: mouse monoclonal LY1C6 (#428017 Calbiochem, Burlington, MA, USA); LC3: rabbit monoclonal D3U4C against LC3A/B (#12741; Cell Signaling Technology), mouse monoclonal (#MI52; MBL International, Woburn, MA, USA); Rab7: rabbit monoclonal D95F2 (#9367; Cell Signaling Technology); ubiquitin: mouse monoclonal P4D1 (#3936; Cell Signaling Technology), mouse monoclonal (#04-263 Millipore, Burlington, MA, USA); Cre: rabbit polyclonal (#69050; Millipore); p62: guinea pig polyclonal (#03-GP62-C; American Research Products, Waltham, MA, USA). CaBP5: Rabbit polyclonal,[27,28] kindly gifted by Françoise Haeseleer (University of Washington, Seattle, WAS, USA); TRPM1: mouse monoclonal 545H5.[29,30]

Mouse eyes were rinsed in PBS, fixed with 4% paraformaldehyde (PFA) in PBS for 45 minutes at room temperature, then dissected. Eyecups were cryoprotected in 26% sucrose in PBS overnight at 4°C, then embedded in OCT. Whole brains were fixed with 4% paraformaldehyde in PBS for 24 hours, cryoprotected as above, and cerebella were embedded in OCT. Ten to 20 μm retina sections or parasagittal cerebellum sections were cut using a cryomicrotome (Fisher Scientific). Sections were washed with PBS before blocking with 10% donkey serum, 5% BSA, 0.5% fish gelatin, and 0.4% triton X-100 in PBS at room temperature for 1 hour. Slides were incubated with primary antibodies diluted 1:50 to 1:100 in blocking buffer overnight at 4°C, washed extensively with PBS, then incubated with 2 μg/mL anti-mouse, anti-guinea pigs, or anti-rabbit secondary antibodies conjugated with Alexa Fluor 488, 555 or 647 (Life Technologies) and 300 nM DAPI in blocking buffer for 1 hour at room temperature, washed with PBS, and mounted with Vectashield anti-fade reagent (Vector Laboratories).

Samples were imaged with a Leica TCS SP5 laser scanning confocal microscope using a 63× oil immersion objective (HC PL APO CS2 63.0x, numerical aperture 1.40; Leica Biosystems, Wetzlar, Germany) and excitation light from a 405 nm diode laser, 488 nm argon laser, and 543/647 nm HeNe lasers. Z-stacks were acquired in 0.1 μm steps and converted to maximum z-projections using LAS AF software (Leica Biosystems). Contrast and brightness were adjusted with ImageJ (National Institutes of Health [NIH], Bethesda, MD, USA) or Photoshop (Adobe, San Jose, CA, USA). For silver nitrate staining, 20 μm sections were stained with 2% silver nitrate (Sigma-Aldrich Corp.) overnight and imaged with the Leica confocal microscope in brightfield mode. All immunostaining images shown are representative examples of two or more experiments, with the following total number of animals: Figure 1, $n = 7$; Figures 2 and 3, 1 month $n = 3$, 3 months $n =$ 13 (control), and 19 (KO), 10 months $n = 12$ (control) and 15 (KO); Figure 4, $n = 3$ to 4; Figure 6, $n = 4$ (control) and 6 to 7 (KO; Figs. 6A, 6B) or 3 (KO; Fig. 6C); Fig. 7, $n = 4$ to 5; Figure 8, $n = 3$ to 6 (control) and $n = 5$ to 6 (KO); Figure 9, $n = 3$ to 5; Fig. 10, $n = 9$ (control) and 13 (KO); and Supplementary Fig. S1, $n = 15$.

Electron Microscopy

Transmission electron microscopy (TEM) was performed as described.[15] Briefly, eyecups were fixed in 3% PFA and 3% glutaraldehyde and postfixed with 1% OsO_4, followed by graded dehydration in ethanol, and gradual infiltration with

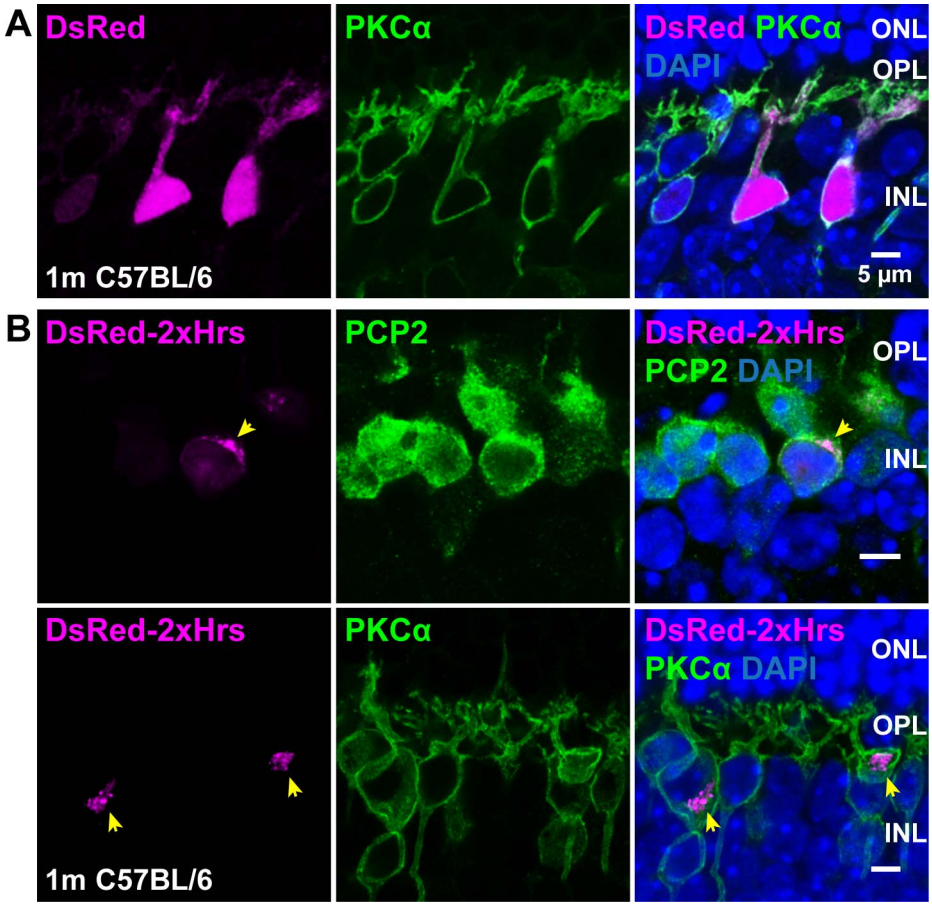

Figure 1. Location of PI(3)P in ON-BCs. DsRed (**A**), or a fusion of DsRed with two tandem repeats of the PI(3)P-specific Hrs FYVE domain (DsRed-2xHrs, [**B**]), were expressed in a random subset of ON-BCs using the Grm6 promoter. Retina sections were immunostained with PCP2 or PKCα antibodies (*green*) to label bipolar cells. The two rows in **B** show examples from two different mice; *yellow arrowheads* indicate PI(3)P-positive membranes in expressing cells.

resin (Embed-812; Electron Microscopy Sciences, Hatfield, PA, USA). Thin sections 80 to 90 nm thick on mesh grids were stained with 2% uranyl acetate and Reynold's lead citrate.

Electroretinography

Animals were dark-adapted overnight, then anesthetized by intraperitoneal injection of ketamine (90 mg/kg) and xylazine (15 mg/kg). A 10 μL drop of 1.25% phenylephrine/0.5% tropicamide was instilled on each eye for mydriasis, and the mouse was placed in a heated (~34°C) holder. A ground electrode was placed under the skin of the forehead, and wire loop electrodes were placed encircling each eye. A drop of hypromellose ophthalmic solution (Goniovisc; Hub Pharmaceuticals, Rancho Cucamonga, CA, USA) diluted 5-fold in PBS to 0.5% hypromellose was placed over each eye to maintain electrical conductivity and corneal hydration. All preparations were performed under dim red light. Electroretinography (ERG) recordings were performed with the UTAS BigShot Visual Electrodiagnostic System (LKC Technologies, Gaithersburg, MD, USA), with flashes delivered by white LED. Responses were recorded at a sampling rate of 2000 Hz with a 60 Hz notch filter used. The mouse holder was placed inside the Ganzfeld chamber and adapted in complete darkness for 7 to 10 minutes before recording. For scotopic measurements, responses to 30 flashes were averaged for intensities in 5 dB increments between −55 dB and −10 dB. Animals then were adapted in constant background white light (30 cd/m^2) for 7 to 10 minutes before photopic recordings; the background light remained on during the recordings. Responses to 60 flashes were averaged for intensities from −10 to 0 dB, and 20 flashes were averaged for 5 and 10 dB. Interstimulus intervals were 3 seconds for flash intensities ≤0 dB, and 5 seconds for intensities >0 dB. Flash intensity units were converted from dB to log[R*/rod] according to a previously determined calibration.[31]

Data were analyzed using custom code in Mathematica v.9.0.1 (Wolfram, Champaign, IL, USA). For baseline subtraction, the mean signal of the 15 ms preceding the flash was subtracted. The a-wave amplitude was measured as the distance between the baseline and the minimum of the first 35 ms following the flash. For b-wave determination, responses were low pass filtered at 55 Hz using the LowpassFilter function (cutoff frequency = 2π 55, kernel = 1000). Amplitudes of b-waves were measured as the distance between the a-wave minimum and the maximum peak of the filtered data between 30 and 120 ms following the flash. Left and right eyes were averaged. Intensity-response data were fit to a linear saturation response function using nonlinear regression (Levenberg-Marquardt algorithm) in Prism v.3.02 (GraphPad, San Diego, CA, USA). To determine whether control and KO b-wave amplitudes are significantly different, best-fit intensity-response curves were generated separately for b-wave data from Vps34$^{fl/fl}$ and Vps34$^{fl/fl}$;Pcp2-Cre animals; and this model was compared to the null hypothesis model (a curve fit to combined Vps34$^{fl/fl}$ and Vps34$^{fl/fl}$;Pcp2-Cre data) using an F

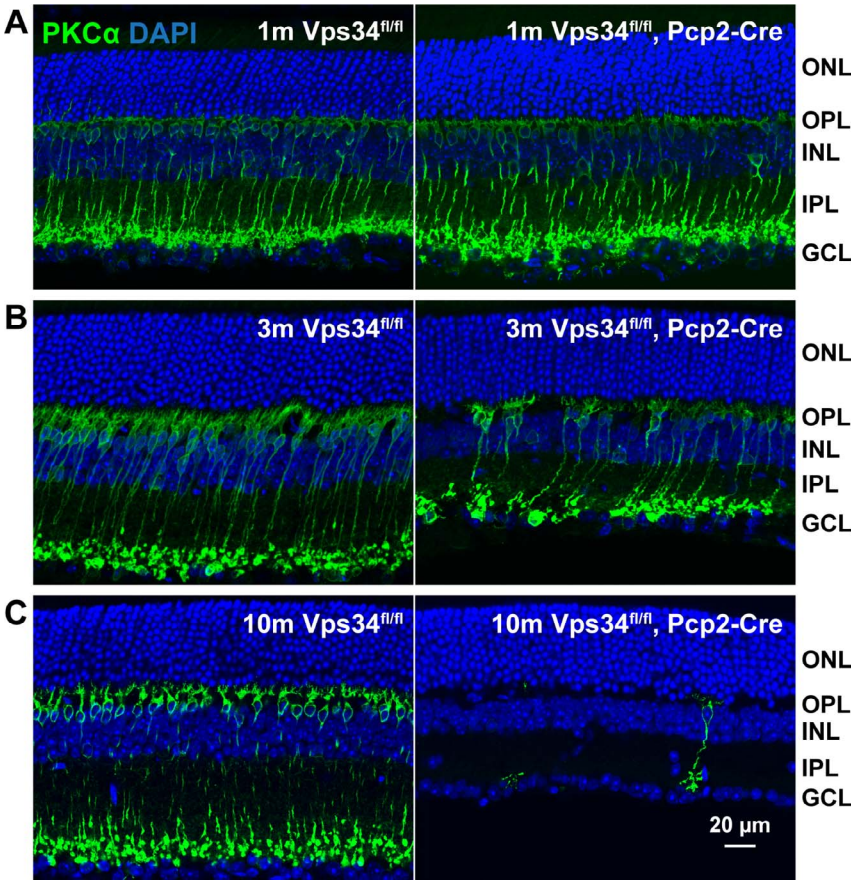

FIGURE 2. Progressive degeneration of rod BCs. Sections from control or Vps34$^{fl/fl}$;Pcp2-Cre retinas were immunostained for the rod BC marker PKCα (*green*) at 1 (**A**), 3 (**B**), or 10 (**C**) months of age. Near complete loss of rod BCs and thinning of the INL and IPL are evident at 10 months. No changes in ONL thickness were observed.

test. Determination of F ratios and calculation of associated *P* values were carried out using Microsoft Excel 2003.

Accelerated Rotarod Test

Rotarod tests were performed at the Baylor College of Medicine Neurobehavioral Core using the RotaRod 47650 NG (Ugo Basile, Gemonio, Italy). 11-week-old Vps34$^{fl/fl}$;Pcp2-cre and Vps34$^{fl/wt}$;Pcp2-cre littermate controls were placed on a horizontal rubber-coated rod for two trials, 30 minutes apart. For each trial, the rotation speed was increased linearly from 4 to 40 revolutions per minute over a 5-minute period, then kept constant at 40 rpm for an additional 5 minutes. The fall latency is the time on the rod before falling off.

RESULTS

Localization of PI(3)P in Internal Membranes of ON-BCs

To visualize PI(3)P-containing membranes specifically in ON-BCs, a plasmid expressing DsRed fused to two tandem repeats of the FYVE domain from Hrs, which binds specifically to PI(3)P,[15,32–34] under control of the ON-BC-specific Grm6 promoter,[23,35,36] was introduced by subretinal injection and electroporation.[24] In contrast to DsRed, which was diffuse throughout the transfected cells (Fig. 1A), DsRed-2xHrs appeared in patches or punctate clusters, primarily in the cell somas (Fig. 1B). Thus, as in other cell types, PI(3)P is readily detectable in ON-BCs and is found primarily in a specific subset of intracellular membranes.

Conditional KO of Vps34

Vps34 is the type III PI 3-kinase primarily responsible for production of PI(3)P.[13,15,37] A BC KO of Vps34 was generated by crossing mice with loxP sites flanking the Vps34 exons encoding the ATP binding domain[13] with a transgenic line that expresses Cre under control of the Pcp2 promoter, which drives expression in rod and cone BCs and cerebellar Purkinje cells.[17–19] In the retina, Cre expression was detected in a subset of BCs, including both rod BCs, identified by PKCα staining, and cone BCs, identified by morphology, stratification, lack of PKCα staining, and expression of Cre (Supplementary Fig. S1). The resulting Vps34$^{fl/fl}$;Pcp2-Cre mice have an in-frame deletion of the ATP binding domain and, thus, ablation of Vps34 catalytic function, but the potential to synthesize a nearly full-length, albeit catalytically inactive, protein in retinal BCs and Purkinje cells.

Progressive Degeneration of Vps34 KO BCs

The retinal layers developed normally in the KO mice, and at 1 month of age, the retinas, including BCs, appeared normal (Figs. 2, 3). However, as they aged, KO mice exhibited a progressive loss of BCs expressing PCP2, accompanied by a thinning of the INL. Rod bipolar cells, identified by PKCα immunostaining, were typically reduced in number by 3 months, and almost completely absent at 10 months (Figs. 2,

Investigative Ophthalmology & Visual Science

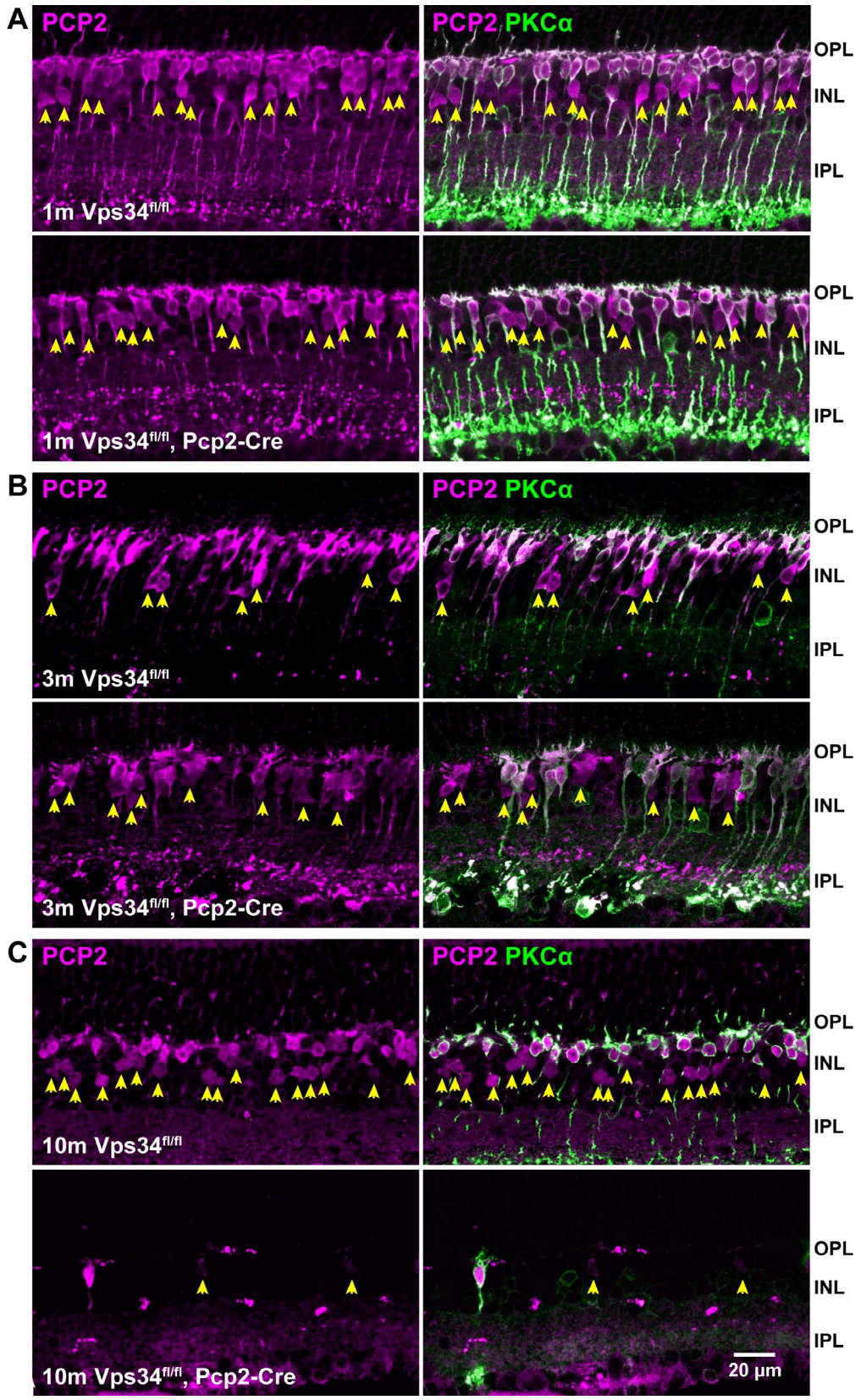

Figure 3. Progressive degeneration of PCP2-expressing cone BCs. Sections from control or Vps34$^{fl/fl}$;Pcp2-Cre retinas were immunostained with antibodies for PCP2 (*magenta*) and PKCα (*green*) at 1 (**A**), 3 (**B**), or 10 (**C**) months. The numbers of rod BCs (*green*) and cone BCs expressing PCP2 (*arrowheads*) were greatly reduced by 10 months.

Investigative Ophthalmology & Visual Science

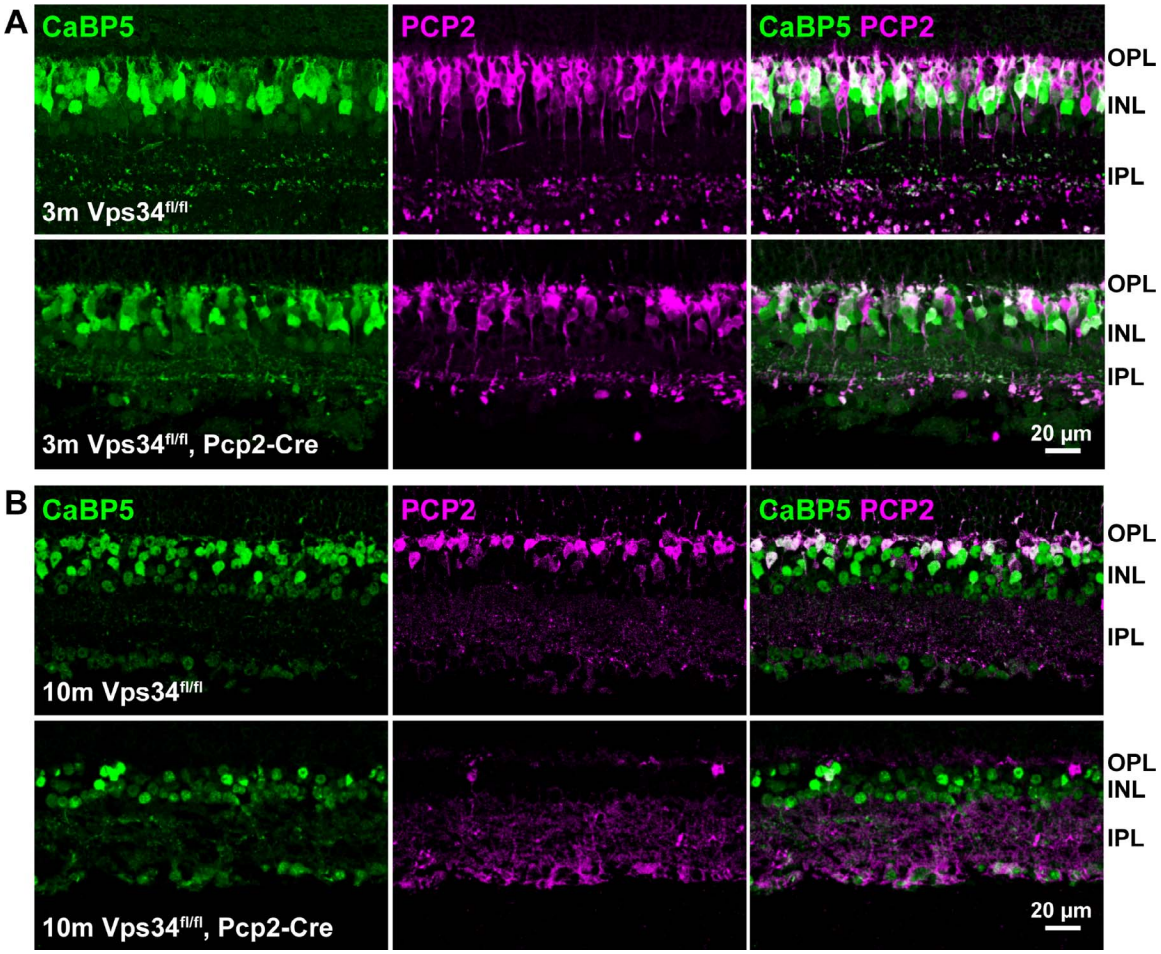

FIGURE 4. Sparing of PCP2-negative cone BCs. Sections were immunostained with antibodies for PCP2 (*magenta*) and CaBP5 (*green*), which is expressed in rod BCs and cone type 5-ON and type 3-OFF BCs. Vps34$^{fl/fl}$ controls and Vps34$^{fl/fl}$;Pcp2-Cre retinas at (**A**) 3 months and (**B**) 10 months. At 10 months, very few PCP2-positive cells remain in Vps34$^{fl/fl}$;Pcp2-Cre retinas, whereas other BCs labeled with CaBP5 were spared.

3). The extent of degeneration at intermediate time points varied greatly among animals (Supplementary Fig. S3). In addition to rod BCs, the Pcp2 promoter also is active in cone type 6 ON-BCs and type 2 OFF-BCs.[16] These cells, identified by the presence of PCP2 and absence of PKCα (arrows, Fig. 3), were also largely absent by 10 months. Cone type 5 ON-BCs and type 3 OFF-BCs, which do not express PCP2,[16] can be identified by lack of PCP2 staining and presence of the calcium-binding protein, CaBP5. Many of these cells still were present, even at 10 months when PCP2-positive cells were nearly completely degenerated (Fig. 4).

The positive b-wave of the ERG is largely due to depolarization of ON bipolar cells and serves as a diagnostic for their function. The BC degeneration in KO mice was accompanied by reduced ERG b-wave amplitudes (Fig. 5). At 2 months, average responses of KO mice were not significantly different from controls. However, 6- to 7-month-old KO mice had significantly reduced scotopic b-waves, reflecting loss of rod-BCs. Photopic responses also were smaller, consistent with loss of rod and cone ON-BCs. Consistent with the variable extent of BC degeneration observed by immunohistochemistry (Supplementary Fig. S3A), the b-wave amplitudes in KO mice also were highly variable, ranging from moderately reduced to completely absent (Supplementary Fig. S3B); two examples are shown on the right in Figure 5A. The a-wave amplitudes were normal at the ages tested, indicating preservation of rod cell function, despite loss of their postsynaptic partners.

Sparing of Other Retinal Neurons and OPL Synapse Structure

Staining for the marker of presynaptic ribbons, ribeye, is predominantly due to ribbons in rod spherules and cone pedicles. Following degeneration of BCs, ribeye immunostaining in the outer plexiform layer was maintained (Fig. 6). Similar results were seen with PKCα (Fig. 6A), which labels rod BC cytoplasm, and TRPM1 (Fig. 6B), which labels somas and dendritic tips of rod and cone ON BCs. These results demonstrate loss of BCs, including their dendrites, but not presynaptic ribbons. Similarly, horizontal cell dendrites, which participate along with bipolar cell dendrites in the rod spherule triad synapses, appeared normal; punctate immunostaining of the horizontal cell marker calbindin in the OPL is closely apposed to ribbon staining in both control and KO mice (Fig. 6C). Horizontal cell bodies also appear to be normal in number (Fig. 6C). Quantification of OPL puncta containing ribeye and calbindin staining (Fig. 6D) is consistent with maintenance of photoreceptor–horizontal cell synapses following BC degeneration.

Similarly, outer nuclear layer (ONL) thickness in the KO mice remained normal, containing 10 to 12 layers of nuclei for at least 10 months, indicating no photoreceptor cell death during that time (Fig. 2). Amacrine cells, labeled with either calretinin or parvalbumin in the INL, appeared to have an approximately normal complement of cell bodies at 3 months,

Investigative Ophthalmology & Visual Science

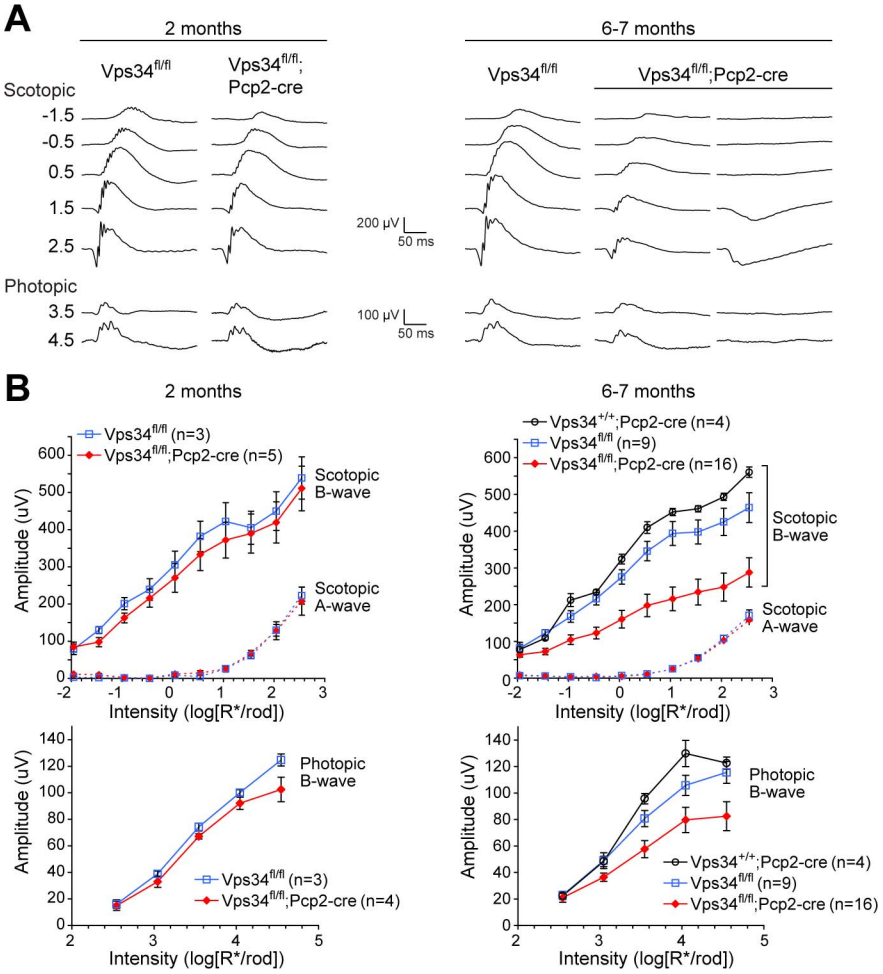

Figure 5. Loss of BC-driven b-wave responses. (**A**) Example recordings from control or Vps34$^{fl/fl}$;Pcp2-Cre KO mice at 2 months (*left*) or 6 to 7 months (*right*). Examples from two 6- to 7-month KO mice are shown to illustrate the variability among animals. (**B**) Aggregate a- and b-wave amplitudes. Amplitudes of b-waves were significantly smaller in the KO at 6 to 7 months, while a-waves were unchanged. *Points* and *error bars* represent means ± SEM, and the number of mice for each genotype is indicated in parentheses. To determine whether control and KO b-wave amplitudes are significantly different, best-fit intensity-response curves were generated separately for b-wave data from Vps34$^{fl/fl}$ and Vps34$^{fl/fl}$;Pcp2-Cre animals. This model was compared to the null hypothesis model (a curve fit to combined Vps34$^{fl/fl}$ and Vps34$^{fl/fl}$;Pcp2-Cre data) using an F test, yielding $P < 0.001$ for both scotopic and photopic b-waves.

though the stratifications of the inner plexiform layer (IPL) were compressed (Fig. 7).

Membrane Processing Defects in Vps34 KO BCs

KO of Vps34 in other cell types leads to defects in autophagosome and endosome processing.[13,15,37,38] In Vps34$^{fl/fl}$ control mice, staining for autophagosome marker proteins LC3 and p62 yields no detectable fluorescent puncta, due to the transient nature of autophagosomes formed under normal conditions (Fig. 8A). In Vps34 KO BCs, large bright puncta accumulate, which are positive for LC3 and p62 (Figs. 8B–D). These puncta also were observed in KO mice with a transgene expressing a fusion of EGFP with LC3 (Fig. 8C). By TEM, large membrane aggregates and other vacuolar-like aberrant membrane structures were observed to accumulate in the INL (Fig. 8E). Such membranes are a characteristic of cells in which autophagosomes can form, but cannot be degraded by fusion with lysosomes.[15]

The LC3-positive puncta also contained ubiquitinated proteins (Fig. 9A), which are characteristic of autophagosomes. Lysosomal marker LAMP1 also accumulated but did not colocalize with the LC3 puncta (Fig. 9B), indicating a defect prior to autophagosome-lysosome fusion. We did not observe accumulation of the early endosome marker Rab5 (data not shown), but accumulation of the late endosomal protein Rab7 in Vps34 KO mice (Fig. 9C) suggests a defect in late endosome processing, again likely due to failure of endosome-lysosome fusion.[15]

Progressive Degeneration of Purkinje Cells

Vps34$^{fl/fl}$;Pcp2-Cre mice also underwent rapid degeneration of cerebellar Purkinje cells (Fig. 10), consistent with Pcp2-Cre expression in these cells. Cerebella were reduced in size (Fig. 10A), and loss of Purkinje cells, identified by PCP2 immunostaining in the Purkinje and molecular layers (ML), was evident at 1 month and complete by approximately 3 months (Fig. 10C). Modified Golgi staining confirmed that the cell bodies in the Purkinje layer were absent (Fig. 10B). Accumulation of puncta containing autophagy marker p62 was observed prior to cell death (Fig. 10D), consistent with the autophagy defect observed in BCs. Vps34$^{fl/fl}$;Pcp2-Cre animals developed an ataxic walking gait around 1 month, which worsened with age. Accelerated Rotarod tests on 11-week mice demonstrated

Investigative Ophthalmology & Visual Science

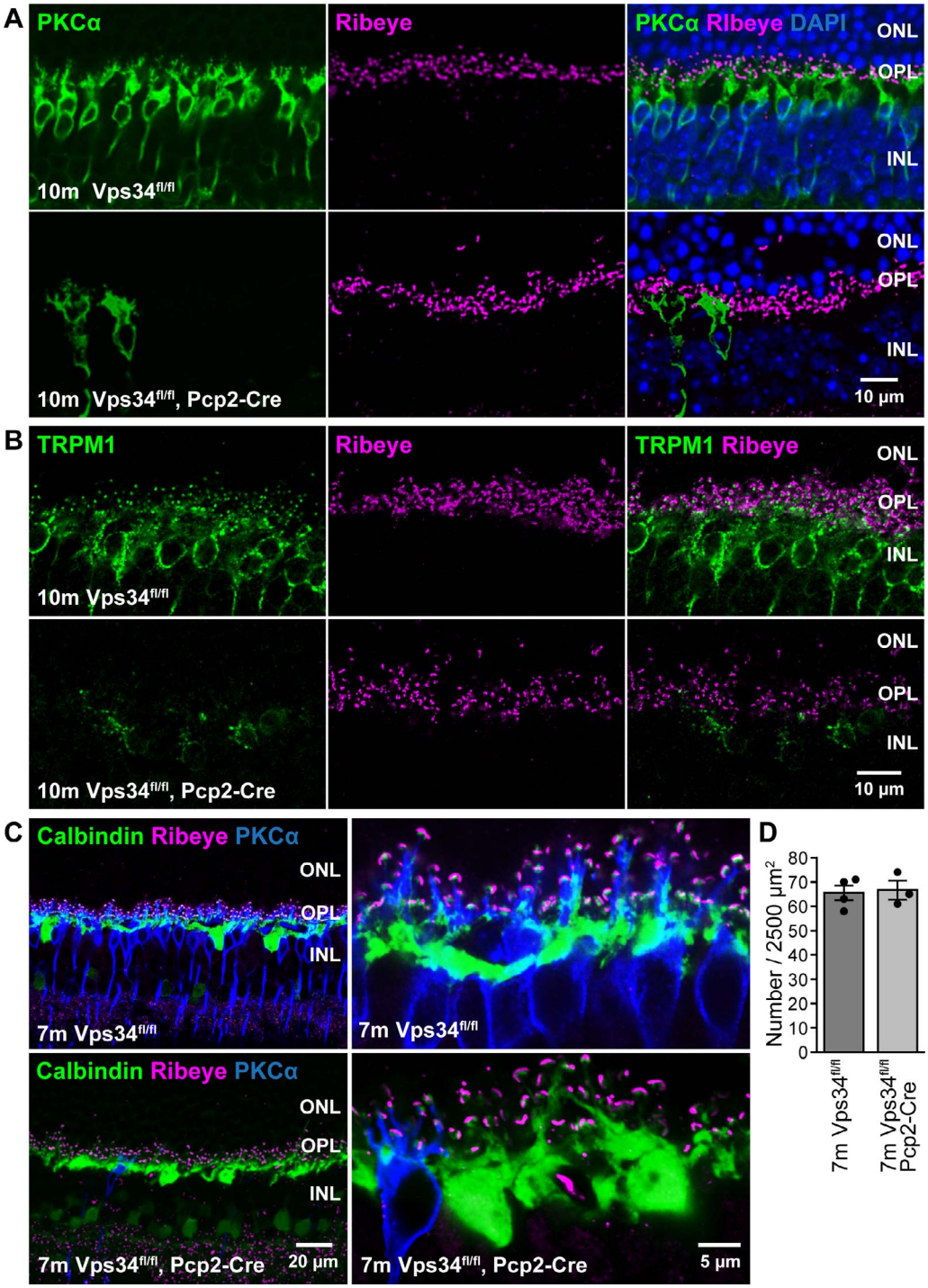

Figure 6. Maintenance of horizontal cells and rod synaptic terminals. (**A**, **B**) Immunostaining for ribeye (*magenta*), a component of the presynaptic ribbon, appears normal in Vps34$^{fl/fl}$;Pcp2-Cre mice at 10 months, when PKCα (*green*, [**A**]) or TRPM1 (*green*, [**B**]) staining indicates near complete loss of ON-BCs. (**C**) Sections triple labeled for calbindin, a horizontal cell marker (*green*), ribeye (*magenta*), and PKCα (*blue*), indicate preservation of horizontal cell dendrites and OPL puncta. (**D**) Quantification of OPL synapses. OPL puncta containing closely-apposed ribeye and calbindin staining were counted in 50 × 50 μm fields from three to four images, each from a different animal.

reduced motor coordination and balance (Fig. 10E), consistent with Purkinje cell degeneration.[39–41]

Discussion

Our results showed that Vps34 KO leads to autophagy defects and degeneration of retinal BCs and Purkinje cells. These findings mirrored results obtained with Vps34 KO in other cell types, including rod photoreceptors,[15] sensory neurons,[13] hepatocytes,[37] and podocytes,[42] and demonstrated the requirement of Vps34 for autophagy in BCs.

In addition to autophagy, Vps34 and PI(3)P have important roles in other membrane trafficking processes, such as endocytosis, endosome processing, and retrograde traffick-

Investigative Ophthalmology & Visual Science

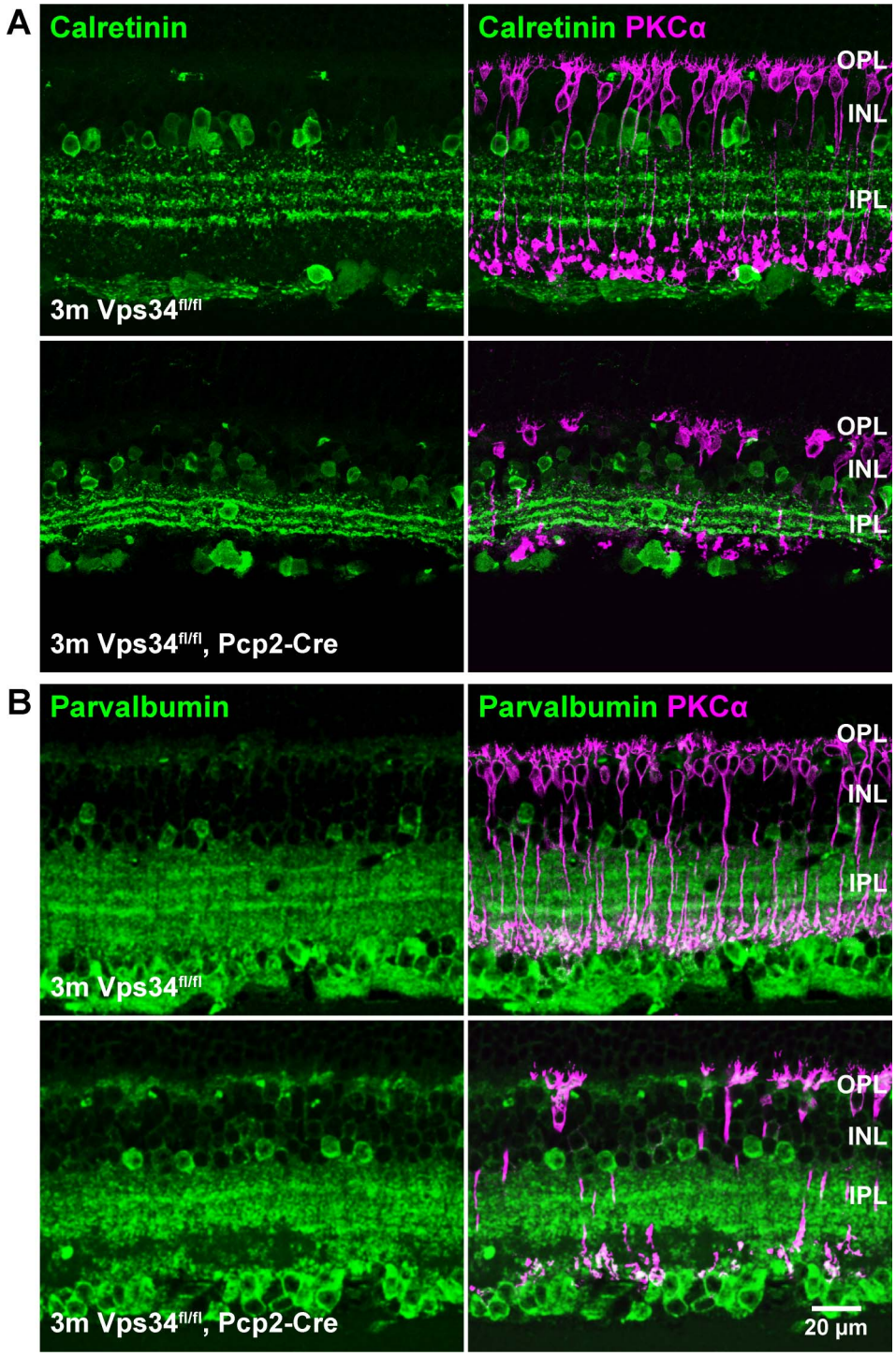

Figure 7. Sparing of amacrine cells. Retina sections were immunostained for AII amacrine cell markers calretinin (**A**) or parvalbumin (**B**). Cell bodies appeared normal in Vps34$^{fl/fl}$;Pcp2-Cre mice at 3 months, though rod BC degeneration was observed with PKCα staining (*magenta*).

ing,[1,2] and defects in these processes likely contribute to a more severe phenotype in Vps34 KO cells.[13,15,42] Consistent with this idea is our observation of ataxia and partial Purkinje cell degeneration by 1 month of age, and complete loss of Purkinje cells by approximately 3 months (see Fig. 10). This result is in contrast to mice with Pcp2-Cre–mediated Purkinje cell KO of the autophagy protein Atg5, which did not develop ataxia until approximately 10 months; at that age they had only partial loss of Purkinje cells.[40]

In addition to producing PI(3)P, the Vps34 protein also participates in various complexes associated with different steps of autophagy and endocytosis.[2,7,8,43–48] The formation of these complexes provides context-specific regulation of local PI(3)P synthesis,[2,48,49] but there also may be other roles for the Vps34 protein. The Vps34 allele[13] used in this study and our previous study in rods[15] encodes an in-frame deletion of the ATP-binding domain, and could potentially produce a near full-length protein lacking kinase activity. The fact that defects in

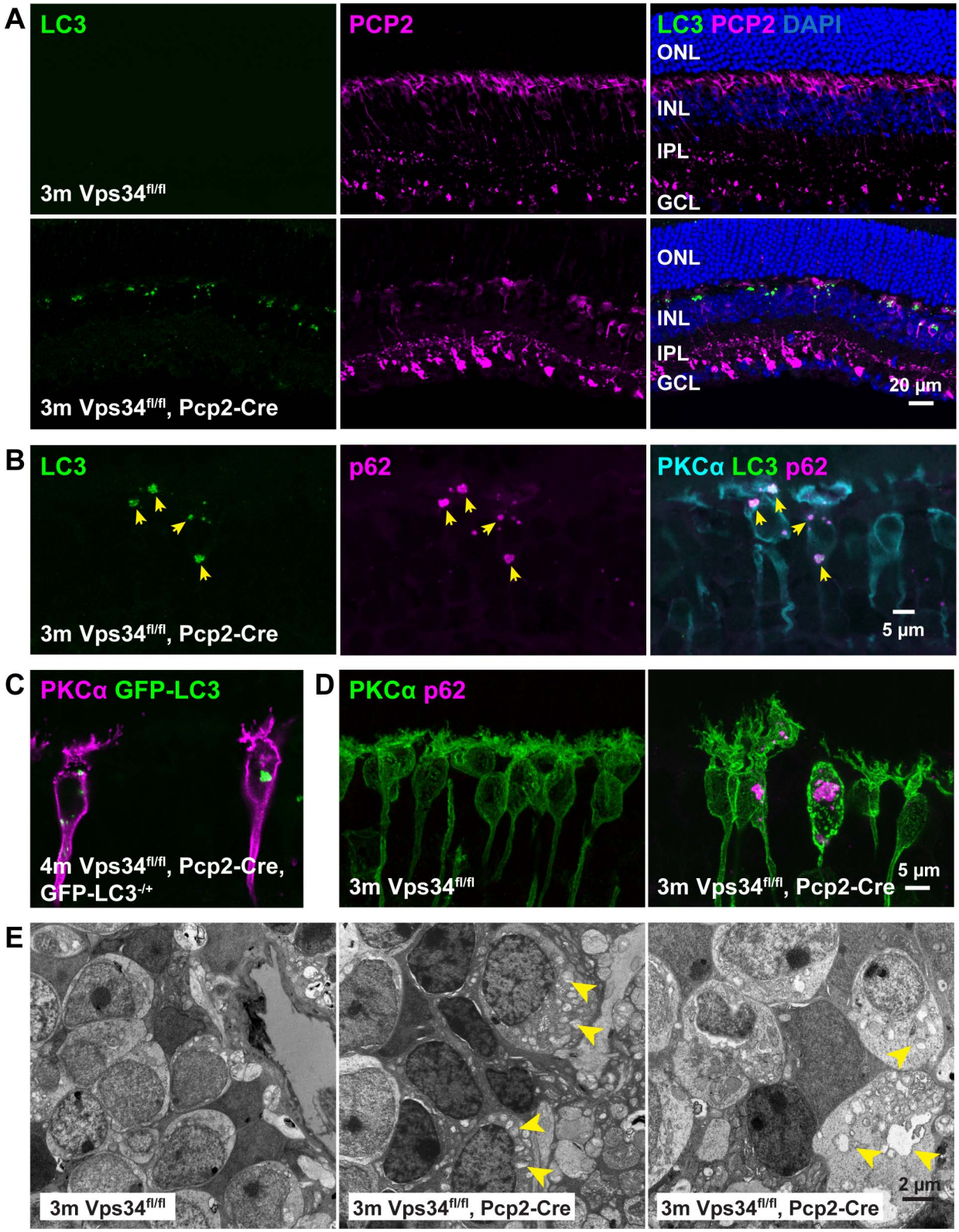

Figure 8. Accumulation of aberrant autophagy-related membranes. (**A**) Sections from 3-month control or Vps34$^{fl/fl}$;Pcp2-Cre KO retinas were immunostained with antibodies for autophagosome markers LC3 (*green*) and PCP2 (*magenta*). Accumulation of large LC3 puncta was observed in the KO retina. (**B**) Costaining with antibodies for LC3 (*green*), p62 (*magenta*), and PKCα (*cyan*) show colocalization of LC3 and p62 in the puncta, and their location in rod BCs. (**C**) Vps34$^{fl/fl}$;Pcp2-Cre;LC3-GFP mice also formed puncta visualized by GFP fluorescence. (**D**) Immunostained sections from control or Vps34$^{fl/fl}$;Pcp2-Cre retinas revealed accumulation of p62 puncta in rod BCs. (**E**) TEM of INL regions from 3-month control and Vps34$^{fl/fl}$;Pcp2-Cre KO retinas show abnormal membrane aggregates in the KO.

Investigative Ophthalmology & Visual Science

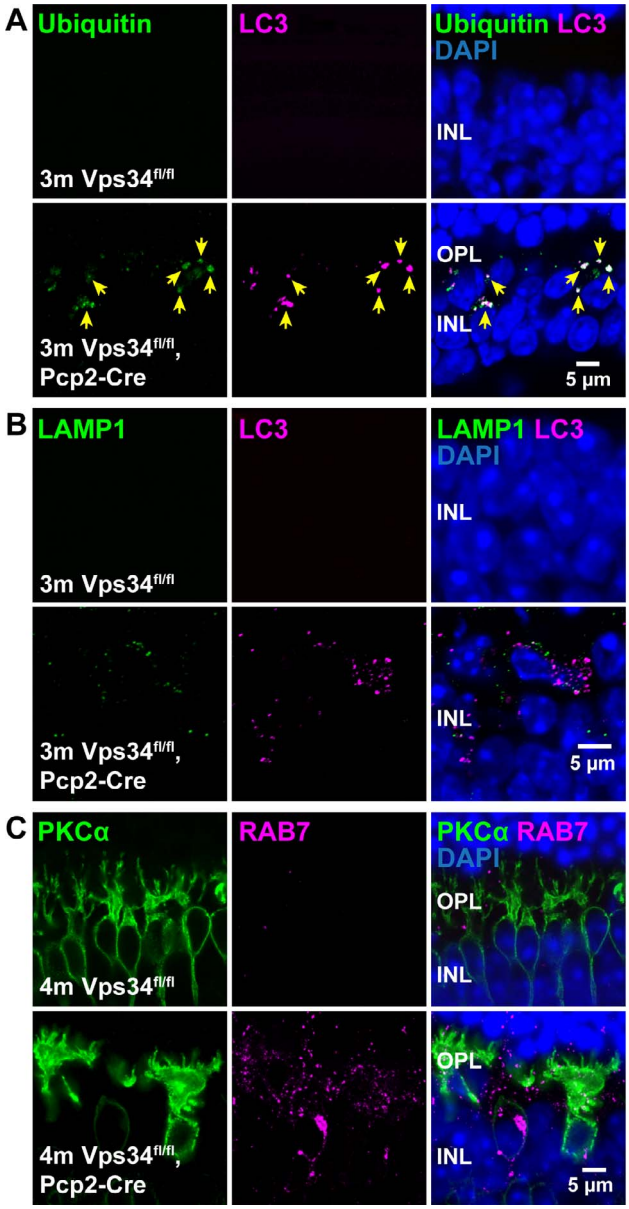

Figure 9. Impairment of autophagolysosome formation and late endosome processing. (**A**) Immunostaining for ubiquitin (*green*) and LC3 (*magenta*) revealed accumulation of ubiquitinated proteins colocalizing with the LC3 puncta in Vps34$^{fl/fl}$;Pcp2-Cre retinas. (**B**) Immunostaining for lysosomal marker LAMP1 (*green*) and LC3 (*magenta*) showed an accumulation of LAMP1-positive puncta, which did not colocalize with LC3, indicative of failure of autophagosome-lysosome fusion. (**C**) Late endosome marker Rab7 immunostaining (*magenta*) also indicated an accumulation of Rab7-positive structures in Vps34$^{fl/fl}$;Pcp2-Cre retinas.

Vps34 KO MEFs were largely rescued by expression of WT Vps34, but not by a kinase-dead Vps34 single amino acid mutant,[38] suggests that lack of PI(3)P synthesis is the major cause of the defects in those cells, and likely in ON-BCs as well.

In autophagy, PI(3)P is canonically thought to be required for recruitment of the Atg12-Atg5-Atg16L complex leading to LC3 lipidation on the autophagophore membrane,[3,7] but the accumulation of LC3 in puncta in Vps34 KO BCs suggests that it is membrane-associated and, therefore, lipidated (see Figs. 8, 9), consistent with PI(3)P-independent lipidation. Therefore, the failure of autophagosome maturation in Vps34 KO ON-BCs is likely due to a requirement of Vps34/PI(3)P in a downstream step (discussed below).

In addition to its role in autophagy, PI(3)P also is present on early and late endosome membranes. The accumulation of Rab7-positive puncta observed in Vps34 KO BCs (see Fig. 9) is consistent with the previously-reported accumulation of activated Rab7 and defective endosome maturation in Vps34 null or knockdown cells,[37,38,50] and suggests a similar defect in late endosome processing in KO BCs.

Vps34 participates in several distinct complexes containing Beclin-1, and among these, complexes containing UVRAG appear to be specifically involved in autophagosome-lysosome fusion and endocytosis.[46–49,51] UVRAG has been shown to interact with phosphoinositides including PI(3)P,[52] and UVRAG knockdown cells have impaired degradative endocytosis.[51] Interestingly, KO of Beclin-1 in Purkinje cells leads to rapid degeneration,[49] within a similar timeframe as the degeneration of Vps34 KO Purkinje cells reported here. Thus, disruption of UVRAG- and Beclin-1–containing Vps34 complexes could account for the multiple defects observed in Vps34 KO BCs and Purkinje cells.

To our knowledge, no previous studies of the role of PI(3)P in retinal BCs have been reported. Like other neurons, BCs rely on endocytosis for recycling of synaptic vesicles at the presynaptic terminals.[53,54] Endocytosis may also have a role in maintaining signaling proteins and ion channels at pre- and postsynaptic sites, though these processes have not been studied in BCs. In other neurons, synaptic vesicle cycling is supported by multiple phosphoinositides,[55] and vesicle recycling is linked to autophagy in presynaptic terminals.[56] The PI(3)P-containing membranes visualized with the DsRed-Hrs probe in WT ON-BCs (see Fig. 1) are likely not autophagy-related membranes, as these are poorly detected in the absence of a treatment, such as rapamycin or chloroquine due to rapid degradation of autophagosomes.[15,57] In other cell types, in the absence of treatment to induce or block autophagy, PI(3)P probes were found mainly on endocytic membranes,[33,49,58] and the same is likely the case here.

A large number of naturally-occurring retinal degeneration alleles/models have been described, which are characterized primarily by degeneration of photoreceptors.[59,60] Some of these have also been shown to have secondary effects on INL neurons, including ON-BCs; for example, Pde6b^{rd1} and Pde6b^{rd10} alleles eventually lead to remodeling and degeneration of BCs following photoreceptor death.[61–63] In this study, we report a novel retinal degeneration paradigm in which BCs are selectively affected and other cell types, as well as OPL rod synapses with horizontal cells, are preserved (see Figs. 4, 6, 7). The apparent maintenance of rod synaptic terminals, despite degeneration of the postsynaptic BCs, is reminiscent of the otherwise normal synapses found in KOs of Gβ5, pikachurin, or ELFN1, in which rod bipolar dendrite invagination into the synapse is impaired.[64–66] In mice null for the transcription factor BHLHB4, rod synapses with horizontal cells also appear to be correctly formed, despite almost complete absence of rod BCs, and as in the Vps34 KO BCs, retina architecture is otherwise normal, apart from thinning of the INL.[67] These results demonstrated that the rod BC dendrites, and the transynaptic interactions they mediate with presynaptic proteins,[66,68] are not required for formation or maintenance of the rod synapse with horizontal cell dendrites. Furthermore, they indicated the dispensability of rod BCs for the health of other retinal neurons and maintenance of retina lamination.

The death of Vps34 KO cells demonstrates the importance of degradative membrane trafficking for cell survival. The specific roles of different membrane trafficking pathways in BCs remain to be determined. However, given the variety of cell types that have now been shown to undergo rapid

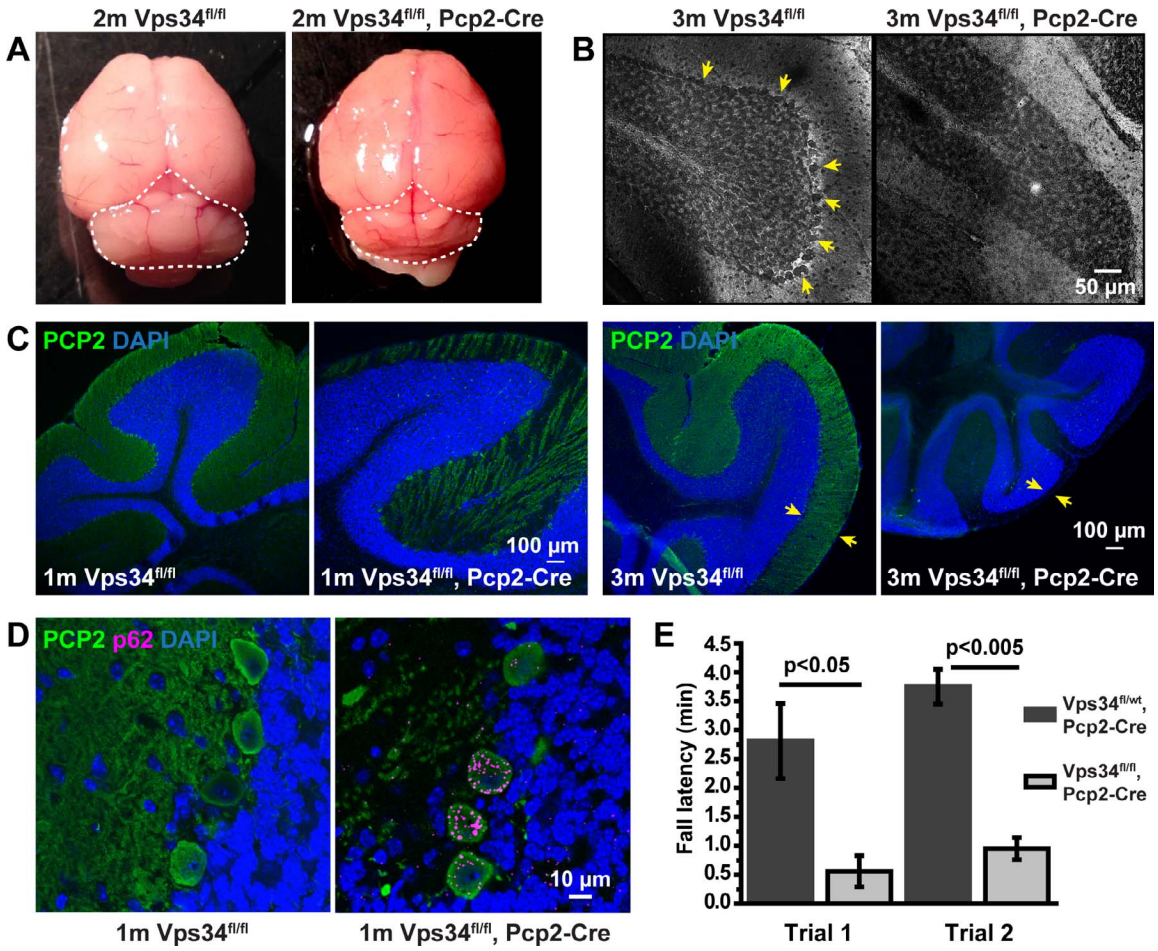

Figure 10. Purkinje cell degeneration. (**A**) The cerebellum (*dashed line*) of the Vps34$^{fl/fl}$;Pcp2-Cre mouse was smaller than that of Vps34$^{fl/fl}$ control mice. (**B**) Parasagittal sections were stained with silver nitrate to visualize Purkinje cell bodies (*arrows*). In the Vps34$^{fl/fl}$;Pcp2-Cre KO mice, Purkinje cells were absent at 3 months. (**C**) Sections were immunostained with an antibody for PCP2 (*green*). In the KO mice, PCP2 labeling of the ML was sparse at 1 month, and completely absent at 3 months, and the thickness of the ML (*arrows*) was reduced. (**D**) Purkinje cells in the KO mice accumulated puncta positive for p62 (*magenta*). (**E**) 11-week control and KO mice were subjected to an accelerated Rotarod test of balance and coordination. KO mice maintained their position on the rod for significantly reduced times, compared to control mice. *Error bars*: Means ± SD; unpaired *t*-test, $n = 3$ for each genotype.

degeneration in the absence of Vps34,[13–15,37,42,69] it is clear that fundamental mechanisms of cell homeostasis are involved.

Acknowledgments

The authors thank Ching-Kang Jason Chen (Baylor College of Medicine) for training in ERG recordings.

Supported by NIH Grants R01-EY025218 and R01-EY026545 and by the Welch Foundation, Q0035 (TGW). The ERG and EM facilities are supported by Core Grant for Vision Research P30 EY002520 from the National Eye Institute (Bethesda, MD, USA). The Neurobehavioral Core is supported by Intellectual and Developmental Disabilities Research Center Grant U54 HD083092 from the Eunice Kennedy Shriver National Institute of Child Health & Human Development.

Disclosure: **F. He**, None; **R.M. Nichols**, None; **L. Kailasam**, None; **T.G. Wensel**, None; **M.A. Agosto**, None

References

1. Lindmo K, Stenmark H. Regulation of membrane traffic by phosphoinositide 3-kinases. *J Cell Sci*. 2006;119:605–614.
2. Backer JM. The intricate regulation and complex functions of the Class III phosphoinositide 3-kinase Vps34. *Biochem J*. 2016;473:2251–2271.
3. Nascimbeni AC, Codogno P, Morel E. Phosphatidylinositol-3-phosphate in the regulation of autophagy membrane dynamics. *FEBS J*. 2017;284:1267–1278.
4. Vanhaesebroeck B, Leevers SJ, Khatereh A, et al. Synthesis and function of 3-phosphorylated inositol lipids. *Annu Rev Biochem*. 2001;70:535–602.
5. Kutateladze TG. Phosphatidylinositol 3-phosphate recognition and membrane docking by the FYVE domain. *Biochim Biophys Acta*. 2006;1761:868–877.
6. Lemmon MA. Membrane recognition by phospholipid-binding domains. *Nat Rev Mol Cell Biol*. 2008;9:99–111.
7. Dikic I, Elazar Z. Mechanism and medical implications of mammalian autophagy. *Nat Rev Mol Cell Biol*. 2018;19:349–364.
8. Hurley JH, Young LN. Mechanisms of autophagy initiation. *Annu Rev Biochem*. 2017;86:225–244.
9. Volinia S, Dhand R, Vanhaesebroeck B, et al. A human phosphatidylinositol 3-kinase complex related to the yeast Vps34p-Vps15p protein sorting system. *EMBO J*. 1995;14:3339–3348.

10. Backer JM. The regulation and function of Class III PI3Ks: novel roles for Vps34. *Biochem J*. 2008;410:1–17.
11. Fagerberg L, Hallström BM, Oksvold P, et al. Analysis of the human tissue-specific expression by genome-wide integration of transcriptomics and antibody-based proteomics. *Mol Cell Proteomics*. 2014;13:397–406.
12. Uhlén M, Fagerberg L, Hallström BM, et al. Tissue-based map of the human proteome. *Science*. 2015;347:1260419.
13. Zhou X, Wang L, Hasegawa H, et al. Deletion of PIK3C3/Vps34 in sensory neurons causes rapid neurodegeneration by disrupting the endosomal but not the autophagic pathway. *Proc Natl Acad Sci U S A*. 2010;107:9424–9429.
14. Wang L, Budolfson K, Wang F. Pik3c3 deletion in pyramidal neurons results in loss of synapses, extensive gliosis and progressive neurodegeneration. *Neuroscience*. 2011;172:427–442.
15. He F, Agosto MA, Anastassov IA, Tse DY, Wu SM, Wensel TG. Phosphatidylinositol-3-phosphate is light-regulated and essential for survival in retinal rods. *Sci Rep*. 2016;6:26978.
16. Euler T, Haverkamp S, Schubert T, Baden T. Retinal bipolar cells: elementary building blocks of vision. *Nat Rev Neurosci*. 2014;15:507–519.
17. Oberdick J, Smeyne RJ, Mann JR, Zackson S, Morgan JI. A promoter that drives transgene expression in cerebellar Purkinje and retinal bipolar neurons. *Science*. 1990;248:223–226.
18. Berrebi AS, Oberdick J, Sangameswaran L, Christakos S, Morgan JI, Mugnaini E. Cerebellar Purkinje cell markers are expressed in retinal bipolar neurons. *J Comp Neurol*. 1991;308:630–649.
19. Slugocka A, Wiaderkiewicz J, Barski JJ. Genetic targeting in cerebellar purkinje cells: an update. *Cerebellum*. 2017;16:191–202.
20. Mattapallil MJ, Wawrousek EF, Chan C-C, et al. The rd8 mutation of the Crb1 gene is present in vendor lines of C57BL/6N mice and embryonic stem cells, and confounds ocular induced mutant phenotypes. *Invest Ophthalmol Vis Sci*. 2012;53:2921–2927.
21. Mizushima N, Yamamoto A, Matsui M, Yoshimori T, Ohsumi Y. In vivo analysis of autophagy in response to nutrient starvation using transgenic mice expressing a fluorescent autophagosome marker. *Mol Biol Cell*. 2004;15:1101–1111.
22. Gimenez E, Montoliu L. A simple polymerase chain reaction assay for genotyping the retinal degeneration mutation (Pdeb rd1) in FVB/N-derived transgenic mice. *Lab Anim*. 2001;35:153–156.
23. Kim DS, Matsuda T, Cepko CL. A core paired-type and POU homeodomain-containing transcription factor program drives retinal bipolar cell gene expression. *J Neurosci*. 2008;28:7748–7764.
24. Matsuda T, Cepko CL. Electroporation and RNA interference in the rodent retina in vivo and in vitro. *Proc Natl Acad Sci U S A*. 2004;101:16–22.
25. Matsuda T, Cepko CL. Analysis of gene function in the retina. *Methods Mol Biol*. 2008;423:259–278.
26. Agosto MA, Anastassov IA, Robichaux MA, Wensel TG. A large endoplasmic reticulum-resident pool of TRPM1 in retinal ON bipolar cells. *eNeuro*. 2018;5:e0143.
27. Haeseleer F, Sokal I, Verlinde CLMJ, et al. Five members of a novel Ca(2+)-binding protein (CABP) subfamily with similarity to calmodulin. *J Biol Chem*. 2000;275:1247–1260.
28. Rieke F, Lee A, Haeseleer F. Characterization of Ca2+-binding protein 5 knockout mouse retina. *Invest Ophthalmol Vis Sci*. 2008;49:5126–5135.
29. Agosto MA, Zhang Z, He F, et al. Oligomeric state of purified transient receptor potential melastatin-1 (TRPM1), a protein essential for dim light vision. *J Biol Chem*. 2014;289:27019–27033.
30. Agosto MA, Anastassov IA, Wensel TG. Differential epitope masking reveals synapse-specific complexes of TRPM1. *Vis Neurosci*. 2018;35:e001.
31. Chen FS, Shim H, Morhardt D, et al. Functional redundancy of R7 RGS proteins in ON-bipolar cell dendrites. *Invest Ophthalmol Vis Sci*. 2010;51:686–693.
32. Gaullier J-M, Simonsen A, D'Arrigo A, Bremnes B, Stenmark H, Aasland R. FYVE fingers bind PtdIns(3)P. *Nature*. 1998;394:432–433.
33. Gillooly DJ, Morrow IC, Lindsay M, et al. Localization of phosphatidylinositol 3-phosphate in yeast and mammalian cells. *EMBO J*. 2000;19:4577–4588.
34. Furutani M, Tsujita K, Itoh T, Ijuin T, Takenawa T. Application of phosphoinositide-binding domains for the detection and quantification of specific phosphoinositides. *Anal Biochem*. 2006;355:8–18.
35. Lagali PS, Balya D, Awatramani GB, et al. Light-activated channels targeted to ON bipolar cells restore visual function in retinal degeneration. *Nat Neurosci*. 2008;11:667–675.
36. Van Wyk M, Pielecka-Fortuna J, Löwel S, Kleinlogel S. Restoring the ON switch in blind retinas: opto-mGluR6, a next-generation, cell-tailored optogenetic tool. *PLoS Biol*. 2015;13:e1002143.
37. Jaber N, Dou Z, Chen J-S, et al. Class III PI3K Vps34 plays an essential role in autophagy and in heart and liver function. *Proc Natl Acad Sci U S A*. 2012;109:2003–2008.
38. Jaber N, Mohd-Naim N, Wang Z, et al. Vps34 regulates Rab7 and late endocytic trafficking through recruitment of the GTPase-activating protein Armus. *J Cell Sci*. 2016;129:4424–4435.
39. Fortier PA, Smith AM, Rossignol S. Locomotor deficits in the mutant mouse, Lurcher. *Exp Brain Res*. 1987;66:271–286.
40. Nishiyama J, Miura E, Mizushima N, Watanabe M, Yuzaki M. Aberrant membranes and double-membrane structures accumulate in the axons of Atg5-null Purkinje cells before neuronal death. *Autophagy*. 2007;3:591–596.
41. Cendelin J, Korelusova I, Vozeh F. The effect of repeated rotarod training on motor skills and spatial learning ability in Lurcher mutant mice. *Behav Brain Res*. 2008;189:65–74.
42. Bechtel W, Helmstädter M, Balica J, et al. Vps34 deficiency reveals the importance of endocytosis for podocyte homeostasis. *J Am Soc Nephrol*. 2013;24:727–743.
43. Christoforidis S, McBride HM, Burgoyne RD, Zerial M. The Rab5 effector EEA1 is a core component of endosome docking. *Nature*. 1999;397:621–625.
44. Kihara A, Kabeya Y, Ohsumi Y, Yoshimori T. Beclin-phosphatidylinositol 3-kinase complex functions at the trans-Golgi network. *EMBO Rep*. 2001;2:330–335.
45. Itakura E, Kishi C, Inoue K, Mizushima N. Beclin 1 forms two distinct phosphatidylinositol 3-kinase complexes with mammalian Atg14 and UVRAG. *Mol Biol Cell*. 2008;19:5360–5372.
46. Liang C, Lee J, Inn K-S, et al. Beclin1-binding UVRAG targets the class C Vps complex to coordinate autophagosome maturation and endocytic trafficking. *Nat Cell Biol*. 2008;10:776–787.
47. Matsunaga K, Saitoh T, Tabata K, et al. Two Beclin 1-binding proteins, Atg14L and Rubicon, reciprocally regulate autophagy at different stages. *Nat Cell Biol*. 2009;11:385–396.
48. Zhong Y, Wang QJ, Li X, et al. Distinct regulation of autophagic activity by Atg14L and Rubicon associated with Beclin 1–phosphatidylinositol-3-kinase complex. *Nat Cell Biol*. 2009;11:468–476.
49. McKnight NC, Zhong Y, Wold MS, et al. Beclin 1 Is required for neuron viability and regulates endosome pathways via the UVRAG-VPS34 complex. *PLoS Genet*. 2014;10:e1004626.

Investigative Ophthalmology & Visual Science

50. Johnson EE, Overmeyer JH, Gunning WT, Maltese WA. Gene silencing reveals a specific function of hVps34 phosphatidylinositol 3-kinase in late versus early endosomes. *J Cell Sci*. 2006;119:1219–1232.
51. Thoresen SB, Marie N, Liestøl K, Stenmark H. A phosphatidylinositol 3-kinase class III sub-complex containing VPS15, VPS34, Beclin 1, UVRAG and BIF-1 regulates cytokinesis and degradative endocytic traffic. *Exp Cell Res*. 2010;316:3368–3378.
52. He S, Ni D, Ma B, et al. PtdIns(3)P-bound UVRAG coordinates Golgi–ER retrograde and Atg9 transport by differential interactions with the ER tether and the beclin 1 complex. *Nat Cell Biol*. 2013;15:1206–1219.
53. Logiudice L, Sterling P, Matthews G. Vesicle recycling at ribbon synapses in the finely branched axon terminals of mouse retinal bipolar neurons. *Neuroscience*. 2009;164:1546–1556.
54. Wan Q-F, Heidelberger R. Synaptic release at mammalian bipolar cell terminals. *Vis Neurosci*. 2011;28:109–119.
55. Lauwers E, Goodchild R, Verstreken P. Membrane lipids in presynaptic function and disease. *Neuron*. 2016;90:11–25.
56. Vanhauwaert R, Kuenen S, Masius R, et al. The SAC1 domain in synaptojanin is required for autophagosome maturation at presynaptic terminals. *EMBO J*. 2017;36:1392–1411.
57. Mizushima N, Yoshimori T, Levine B. Methods in mammalian autophagy research. *Cell*. 2010;140:313–326.
58. Varnai P, Balla T. Live cell imaging of phosphoinositide dynamics with fluorescent protein domains. *Biochim Biophys Acta*. 2006;1761:957–967.
59. Chang B, Hawes NL, Hurd RE, Davisson MT, Nusinowitz S, Heckenlively JR. Retinal degeneration mutants in the mouse. *Vision Res*. 2002;42:517–525.
60. Veleri S, Lazar CH, Chang B, Sieving PA, Banin E, Swaroop A. Biology and therapy of inherited retinal degenerative disease: insights from mouse models. *Dis Model Mech*. 2015;8:109–129.
61. Strettoi E, Pignatelli V. Modifications of retinal neurons in a mouse model of retinitis pigmentosa. *Proc Natl Acad Sci U S A*. 2000;97:11020–11025.
62. Marc RE, Jones BW, Anderson JR, et al. Neural reprogramming in retinal degeneration. *Invest Ophthalmol Vis Sci*. 2007;48:3364–3371.
63. Phillips MJ, Otteson DC, Sherry DM. Progression of neuronal and synaptic remodeling in the rd10 mouse model of retinitis pigmentosa. *J Comp Neurol*. 2010;518:2071–2089.
64. Rao A, Dallman R, Henderson S, Chen C-K. Gβ5 Is required for normal light responses and morphology of retinal ON-bipolar cells. *J Neurosci*. 2007;27:14199–14204.
65. Sato S, Omori Y, Katoh K, et al. Pikachurin, a dystroglycan ligand, is essential for photoreceptor ribbon synapse formation. *Nat Neurosci*. 2008;11:923–931.
66. Cao Y, Sarria I, Fehlhaber KE, et al. Mechanism for selective synaptic wiring of rod photoreceptors into the retinal circuitry and its role in vision. *Neuron*. 2015;87:1248–1260.
67. Bramblett DE, Pennesi ME, Wu SM, Tsai M-J. The transcription factor Bhlhb4 is required for rod bipolar cell maturation. *Neuron*. 2004;43:779–793.
68. Orlandi C, Omori Y, Wang Y, et al. Transsynaptic binding of orphan receptor GPR179 to dystroglycan-pikachurin complex is essential for the synaptic organization of photoreceptors. *Cell Rep*. 2018;25:130–145.
69. Reifler A, Li X, Archambeau AJ, et al. Conditional knockout of Pik3c3 causes a murine muscular dystrophy. *Am J Pathol*. 2014;184:1819–1830.

Investigative Ophthalmology & Visual Science